Brazilian Journal of Physics
ISSN: 0103-9733
luizno.bjp@gmail.com
Sociedade Brasileira de Física
Brasil

Tourinho, F.A.; Campos, A.F.C.; Aquino, R.; Lara, M.C.F.L.; Silva, G. J. da; Depeyrot, J.
Surface charge density determination in electric double layered magnetic fluids
Brazilian Journal of Physics, vol. 32, núm. 2B, junio, 2002, pp. 501-508
Sociedade Brasileira de Física
Sâo Paulo, Brasil

Available in: http://www.redalyc.org/articulo.oa?id=46413505008

- How to cite
- Complete issue
- More information about this article
- Journal's homepage in redalyc.org

Scientific Information System
Network of Scientific Journals from Latin America, the Caribbean, Spain and Portugal
Non-profit academic project, developed under the open access initiative

Surface Charge Density Determination in Electric Double Layered Magnetic Fluids

F.A. Tourinho[1], A.F.C. Campos[1], R. Aquino[1], M.C.F.L. Lara[2],
G. J. da Silva[2], and J. Depeyrot[2]
[1] *Complex Fluids Group, Instituto de Química*
Universidade de Brasília, CP 04478, 70919-970 Brasília (DF), Brazil
[2] *Complex Fluids Group, Instituto de Física*
Universidade de Brasília, CP 04455, 70919-970 Brasília (DF), Brazil

Received on 3 December, 2001

We analyze potentiometric and conductimetric measurements, simultaneously performed in several complex systems (Brönsted acid-base-type). The results show an excellent agreement between reported and obtained values of the dissociation constants of the involved equilibria. A similar analysis is proposed to account, in electric double layered magnetic fluids (EDL-MF), for the charging of the particle surface based on a proton transfer proccess at the interface with the bulk dispersion. This model allows to relate the pH dependence of the phase diagram to the variations of the nanoparticle surface charge density, which leads to a useful method to monitor the colloidal stability of EDL-MF.

I Introduction

Electric Double Layered Magnetic Fluids (EDL-MF) are ultrastable colloidal dispersions of spinel ferrite type nanoparticles electrostatically dispersed in water [1]. The principle of stabilization is to counterbalance the van der Waals and magnetic dipolar attractions and the screened electrostatic repulsions between particles, through a proton transfer mechanism [2], [3] between the bulk dispersion and the particle surface, which creates an adjustable charge density. Modifications in the particle interactions induced by variations of ionic strength [4], temperature [5] or magnetic field [6], may lead to phase transitions, either reversible as liquid-gas-like or irreversible as flocculation. Moreover, the stability of EDL-MF based on maghemite particles has been investigated as a function of pH [7] at room temperature and at constant ionic strength. As the pH controls the surface charge density, interparticle interactions also may be tuned through pH variations and the authors observed a thixotropic gel phase between the sol phase one and the flocculation zone.

Very recently, we showed that simultaneous potentiometric and conductimetric measurements are an excellent tool to determine the superficial density of charge in EDL-MF [3]. The results evidenced the EDL-MF systems behave as a mixture of strong acid and weak diprotic, the bulk dispersion and particle surface, respectively. The surface charge of the particles is generated through the aquation reactions of superficial metal ions which undergo hydrolysis, leading to three kind of superficial sites. The analysis of equilibria involved between the particle surface and the bulk dispersion allows to determine the pH dependence of the surface charge density and to control the colloidal stability of the magnetic sol. Furthermore, measurements performed in EDL-MF based on manganese ferrite nanoparticles of two different diameteres [8] showed that surface charge density depends on the nanoparticle size. Indeed, the existence of surface defects in smaller nanoparticles leads to a reduced saturation value of the surface charge density.

In the present work, our potentiometric and conductimetric approach is applied in the case of well known weak and strong acid mixtures and the dissociation constants involved in such equilibria are obtained. Then, using the same procedure, the acid-base behavior of the surface nanoparticle is investigated and the superficial density of charge is determined for EDL-MF samples based on cobalt [3] and manganese ferrite nanoparticles. In this context, our paper is divided as follows. The second section presents a brief description of proton transfer mechanism in acid-base Brönsted equilibria and results of simultaneous potentiometric and conductimetric titrations are discussed in the case of both solution mixtures of nitric acid with tartaric one and with dihydrate EDTA sodium salt. In the third section, based on phenomenological considerations, we show how the formalism of complex equilibria, involving amphoteric species, can be applied in the case of acid-base properties of nanoparticle surface in EDL-MF, in order to obtain the quantitative pH dependence of the surface charge density. Finally, our titration results are presented and discussed. As an example, we will show how the existence of a thixotropic gel phase can be related to the pH-dependence of the surface charge density.

II Strong and weak acids mixtures: potentiometric and conductimetric approach

II.1 General description

A typical polyfunctional acid H_nA in aqueous media may undergo the following dissociation reactions:

$$H_nA + H_2O \xrightleftharpoons{pK_1} H_3O^+ + H_{(n\text{-}1)}A^- \quad (1)$$

$$H_{(n\text{-}1)}A^- + H_2O \xrightleftharpoons{pK_2} H_3O^+ + H_{(n\text{-}2)}A^{2-} \quad (2)$$

$$\vdots \qquad\qquad\qquad\qquad \vdots$$

$$HA^{(n\text{-}1)\text{-}} + H_2O \xrightleftharpoons{pK_n} H_3O^+ + A^{n\text{-}}. \quad (3)$$

The concentration of each specie depends on the pH and can be expressed using the total molar concentrations of all species C_T, and the molar fraction of each one α_n, where n denotes the number of associated protons:

$$[H_nA] = \alpha_n C_T, \quad \left[H_{(n-1)}A^-\right] = \alpha_{(n-1)}C_T, \quad \ldots \quad \left[A^{-n}\right] = \alpha_0 C_T. \quad (4)$$

The denominator in all α_n value expressions takes the form:

$$[H_3O^+]^n + K_1[H_3O^+]^{(n-1)} + K_1K_2[H_3O^+]^{(n-2)} + ... + K_1K_2...K_n, \quad (5)$$

where K_1, $K_2 \ldots K_n$ are the thermodynamical equilibria constants of H_nA and pK = -log K. The numerator for α_0 is the last term in the denominator; for α_1 it is the next to the last, and so forth. In simple cases, as for example a mixture of strong and weak monoprotic acids, C_T and the pK's values relative to the weak acid are generally obtained from potentiometric measurements. This procedure is based on a neutralization reaction in which an acid (or a mixture of them) reacts with an equivalent amount of base. By constructing a typical titration curve, plotting the pH as a function of the volume of standard base solution, one can determine, from the inflexions in the mono(bi)-log behavior, the stoichiometric points (equivalence points), which give the volume of standard base corresponding to the neutralization of each proton. Nevertheless, in the case of a mixture of strong and weak polyprotic acids, the pH breaks in the titration curve is not well defined when the difference between the sucessive pK's is inferior to 4 or when the pK is superior to 8 [9]. However, we will show, for the first time in the literature, that in such cases, simultaneous potentiometric and conductimetric titrations are an excellent tool to obtain the equivalence points. Then, C_T is determined using the equation of mass balance. Moreover, the thermodynamical constants can be obtained according to the Henderson-Hasselbach [10] equation which writes:

$$pH = pK_n + \log \frac{[A^{-n}]}{[HA^{-(n-1)}]} \quad (6)$$

in the case of general equilibrium (3). Thus, when $[HA^{-(n-1)}] = [A^{-n}]$, the pH is equal to the pK.

II.2 Experimental

II.2.1 Potentiometric and conductimetric measurements

The potentiometric determination of a solution pH is based on the measurement of the potential difference between the cell made of a glass electrode sensitive to hydrogen ion activity and a typical silver-silver chloride reference electrode (E^0 = 0.199 V vs. SHE – Standard

Hydrogen Electrode). The potential of the glass electrode, which arises due to a complex process at the interface of the glass membrane and is proportional to the pH, is measured using a potentiostat. The direct measurement of the pH is obtained after the calibration of the apparatus in the acidic and basic pH ranges, using standard buffers of pH equal to 4 and 7 respectively. The electrical conductivity κ of a solution is a result of the contribution of all charged species in the medium. It can be determined indirectly by measuring the corresponding conductance of the solution and the cell constant which depends on the geometry of the experimental setup. The cell constant has been obtained by measuring the conductivity of a standard solution of potassium chloride (KCl) 3 mol L^{-1} of known conductivity. During the titrations the measurements are performed only once the system reaches the equilibrium.

II.2.2 Mixture of nitric and tartaric acids

A solution of tartaric acid is mixed with concentrated nitric acid in order to obtain a solution pH approximately equal to 2. Then, using an electronic burette Metrohm 715 dosimat, 40 mL of the resulting mixture is titrated with a standard sodium hydroxide (NaOH) solution 0.120 mol / L. The potentiometric readings were performed with a Metrohm 713 potentiometer (precision of 0.1 mV or 0.001 units of pH) with a combined electrode (Metrohm 6.0222.100) and a resistence thermometer (Pt 100). The conductimetric measurements were carried out using a conductometer (Metrohm 712) with an imersion-type measuring cell (Metrohm 6.0901.110). As a common procedure in analytical chemistry, all titrations were repeted two times. All reagents used in this work are of analytical grade from Aldrich or Merk.

II.2.3 EDTA Titration

A solution of dihydrate EDTA sodium salt ($Na_2H_2Y{\cdot}2H_2O$) is prepared and the pH solution is adjusted to 4.3. 40 mL of this solution is titrated with standard sodium hydroxide (NaOH) solution 0.120 mol / L using the same apparatus described previously.

II.3 Results and discussion

II.3.1 Mixture of nitric and tartaric acids

Figure 1 exhibits the potentiometric and conductimetric titrations obtained for the mixture of nitric (strong) and tartaric (weak) acids and shows three distinct regions defined by two equivalence points (EP_1 and EP_3). The meaning of these equivalence points can be described as follows. In the region 1, as the titrant volume increases, the conductivity strongly decreases until the first equivalence point EP_1, due to the complete neutralization of free H_3O^+ ions (from the strong acid) of high specific molar conductivity, substituted by Na^+ ions of lower specific molar conductivity introduced by the titrant. Thus, we assign the first equivalence point to the titration of the nitric acid. The second region corresponds to the tartaric acid titration and in this pH range, the conductivity increases slightly due to the apparition of ionic species in the medium by neutralisation of the 2 protons of tartaric acid. The tartaric acid being diprotic, EP_3 is related to the neutralization of the second proton. As it can be seen in Fig. 1, the equivalence point EP_2 relative to the first proton is not evidenced due to the pK's values close one to another and the titration of the second proton therefore begins before the complete neutralization of the first one. In the region 3, the conductivity increases due to the excess of base, with a lower rate than the decrease one observed in the first region, since the specific molar conductivity of OH^- ions is smaller than that of H_3O^+ ions. Then, EP_1 and EP_3 are determined by using the technique of graphical direction lines [11] and EP_2 can be calculated by the semi-sum of EP_1 and EP_3, since the titrant volume must be equal to titrate each proton of the diprotic acid. Hence, table 1 lists the pK_1 and pK_2 values deduced using the Henderson-Hasselbach equation, in excellent agreement with reported ones [12]. One can note that from the single potentiometric measurements it would be impossible to graphically determine pK_1 and pK_2 since the first equivalence point is not evidenced.

Table 1. Determined pK's values of tartaric acid titration.

	pK_1	pK_2
This Work	3.02 ± 0.15	4.28 ± 0.22
Reported values [12]	3.04	4.37

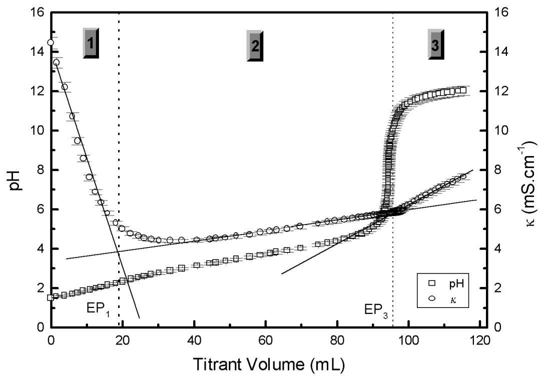

Figure 1. Simultaneous conductimetric-potentiometric titration curves of the mixture of nitric and tartaric acids. The region indexed 1, 2 and 3 correspond to the strong acid titration (HNO_3), the tartaric acid and the base excess respectively. EP_1 and EP_3 are determined by the technique of graphical directions lines.

II.3.2 EDTA Titration

Figure 2 shows the potentiometric and conductimetric titrations obtained in this case, and, also denotes three distincts regions. The region 1 corresponds to the titration of the weak acid H_2Y^{2-} and the conductivity slightly decreases. At EP_1, the H_2Y^{2-} specie is completely reacted. Then, the second region corresponds to the HY^{3-} specie titration until EP_2 leading to the formation of Y^{4-} specie. These results show that the successive decreases of the solution conductivity are related to the respective decreases of the specific molar conductivity of the species H_2Y^{2-}, HY^{3-} and Y^{4-}. Although in the sequence of the formed species the net charge increases, this could be due to the hydrodynamic radius of the ion which is larger, reducing therefore the ion mobility. In the region 3, the conductivity increases due to the excess of base, as discussed in the section II.3.1.

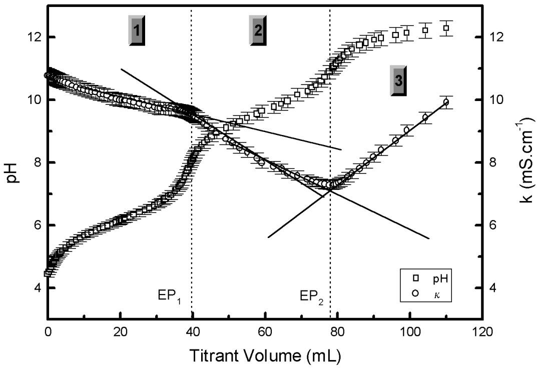

Figure 2. Simultaneous conductimetric-potentiometric titration curves of the dihydrate of the EDTA sodium salt titration. The regions 1 and 2 refer to the titration of H_2Y^{2-} and HY^{3-} species, respectively. The region 3 corresponds to the excess of base titrant. The equivalence points are determined by the technique of graphical directions lines.

From a quantitative point of view, the difference between the two equivalence points EP_1 and EP_2 corresponds to the volume of titrant to neutralize one proton (see 10 or 12). Thus, the graphically determined value of pK_3 and pK_4 of EDTA are listed in table 2 and compared with reported ones.

Table 2. Determined pK_3 and pK_4 values of EDTA.

	pK_3	pK_4
This Work	6.17 ± 0.15	9.80 ± 0.40
Reported values [12]	6.16	10.30

II.3.3 Partial Conclusions

The results presented in section II show that simultaneous potentiometric and conductimetric measurements are a good tool to quantitatively characterize complex systems (Brönsted acid-base-type) since it allows the determination of the stoichimotric points and the chemical equilibria constants. In the following section, we will show that the same measurements are fundamental to investigate the mechanism for the charging of the particle surface based on a proton transfer proccess at the interface with the bulk dispersion. Indeed, EDL-MF behave as a mixture of strong and weak diprotic acids and both the difference between the sucessive pK's is inferior to 4 and the second pK is superior to 8 [3].

III Application to EDL-MF

III.1 The Model

Experimentally, it is well known that stables sols of EDL-MF can be obtained only for acidic or basic medium. In neutral medium, close to the point of zero charge (PZC), the system flocculates [13]. These phenomenological considerations reveal the pH-dependence of the surface charge density of the particles and it is well known that at low (high) pH values the particles are positively (negatively) charged. Moreover in EDL-MF, the superficial particles sites, occupied by transition metals ions, can undergo hydrolysis reactions [14] according to the schematic and simplified equilibrium:

$$\equiv M^{n+} + H_2O \ \rightleftharpoons \ \equiv M, H_2O^{n+} \tag{7}$$

We therefore assume that the following hydrolysis reactions:

$$\equiv MOH_2^{+} + H_2O \rightleftharpoons \equiv MOH + H_3O^{+}{}_{(aq)} \tag{8}$$

$$\equiv MOH + H_2O \rightleftharpoons \equiv MO^{-} + H_3O^{+}{}_{(aq)}\ , \tag{9}$$

are responsible [3,15] for the formation of the superficial charge of the particles in the colloidal dispersion. In such model, the particle surface behaves as a diprotic Brönsted acid, leading to three kinds of surface sites where most of them are $\equiv MOH_2^+$ in strong acidic medium, $\equiv MO^-$ in strong basic medium and $\equiv MOH$, the intermediate amphoteric sites, in the pH_{PZC} region. It is important to point out that this model is in good agreement with a surface charge density positive for $pH < pH_{PZC}$ and negative for $pH > pH_{PZC}$ (see Fig. 3). We therefore express the superficial density of charge as:

$$\sigma_0 = \frac{F}{A} V(\ [MOH_2^+] - [MO^-]\ )\ , \qquad (10)$$

where F is the Faraday constant, A the total surface area of particles is dispersion and V the volume of the dispersion. If C_T is the total concentration of superficial sites and α_n the molar fraction of each one, where n denotes the number of associated protons, (10) writes:

$$\sigma_0 = \frac{F}{A} V\,(\alpha_2 - \alpha_0)\,C_T. \qquad (11)$$

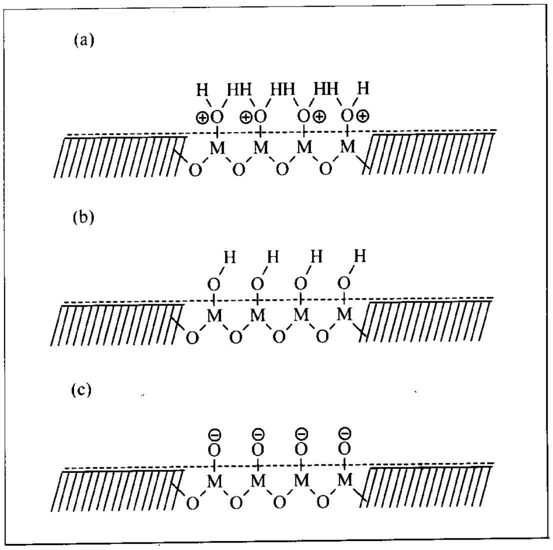

Figure 3. Schematic description of the particle surface as a function of the medium. (a) refers to strong acidic medium where the surface sites are completely protonated and the superficial density of charge is saturated. (b) is related to the neutral medium. In this region, most of the superficial sites are amphoteric and the charge is minimal leading to an flocculation zone. (c) refers to the strong basic medium. The surface sites are negatively charged and the superficial density of charge is saturated. In both (a) and (c) regions the EDL-MF is a stable sol.

Then, using the relation between the hydronium concentration and the pH, the surface charge density can be written as a function of pH:

$$\sigma_0 = \frac{F}{A} V \left(\frac{10^{-2pH} - K_1 K_2}{10^{-2pH} + K_1 10^{-pH} + K_1 K_2} \right) C_T. \qquad (12)$$

In the present work, C_T and the constants pK_1 and pK_2 corresponding to equilibria (8) and (9) respectively, are experimentally determined. Moreover, the total surface area of particles can be obtained by using X-rays diffraction results.

III.2 Experimental

The elaboration of two different EDL-MF samples is carried out using the usual procedure [13]. $CoFe_2O_4$ and $MnFe_2O_4$ oxides nanoparticles are prepared through hydrothermal coprecipitating aqueous solutions of $Co(NO_3)_2$-$FeCl_3$ and $MnCl_2$-$FeCl_3$, respectively, in alkaline medium. Then the particles are conveniently peptized in acidic medium by adjustment of the ionic strength, resulting in stable sols of high quality.

The mean nanoparticle sizes are determined using X-rays diffraction spectra recorded from powder samples and are found equal to 12.0 nm ($CoFe_2O_4$) and 9.0 nm ($MnFe_2O_4$) leading to EDL-MF samples labeled A and B respectively.

Simultaneous potentiometric and conductimetric titrations of 40 mL of each sample (volume fraction $\Phi_A = 1.46\%$ and $\Phi_B = 0.81\%$ corresponding to $1.7\text{x}10^{22}$ and $2.1\text{x}10^{22}$ particles per m^3, respectively) are performed using titrant solutions of sodium hydroxide 0.106 mol L^{-1} and 0.088 mol L^{-1} for samples A and B, respectively. All titrations are repeated two times. Simultaneous potentiometric and conductimetric readings are carried out using apparatus and conditions described in section II.2.2. Moreover our potentiometric measurements are obtained here using a pH glass double-junction electrode (Metrohm 6.0255.100), which includes a salt bridge in order to avoid the direct contact of the colloidal solution to the glass membrane.

III.3 Results and Discussion

Figure 4 exhibits typical simultaneous potentiometric and conductimetric titration results obtained for sample B. These experiments performed in the same conditions for sample A have been presented and commented in a previous paper [3]. The titration curves obtained for manganese based ferrofluid (sample B) follow the same qualitative behavior. As in Figs. 1 and 2, the shape of the curve indicates that EDL-MF sample behave as a mixture of strong and weak diprotic acids. Three distinct regions can be observed and labeled 1, 2 and 3. The region 1 ends at EP_1 and is relative to the strong acid titration (free H_3O^+ ions of the bulk dispersion). The second region corresponds to a weak diprotic acid titration, in our case, the particle surface. According to equilibrium reactions (8) and (9), the corresponding surface sites $\equiv MOH_2^+$ and $\equiv MOH$ are successively titrated therefore allowing the determination of two equivalence points: EP_2 and EP_3, respectively. Until EP_2, that corresponds to $\equiv MOH_2^+$ sites titration, the contribution of superficial protons to the total conductivity is negligible due to the mass of the particles. Thus, the conductivity simultaneously increases slightly since the concentration of Na^+ from the titrant increases. At EP_2, the particle surface becomes amphoteric and neutral ($\equiv MOH$ sites). Then, until EP_3 the second superficial proton is titrated. In this regime, a very small decrease of the conductivity is observed, and could be assigned to adsorption of Na^+ ions onto the surface. Finally, the region 3 is related to the base excess. As used in section II.3.1 the equivalence points EP_1 and EP_3 are determined by using the technique of graphical direction lines and the second equivalence point EP_2 can be calculated by the semi-sum of EP_1 and EP_3. Then, pK_1 and pK_2 values are obtained using the Henderson-Hasselbach equation. Moreover, the whole superficial sites concentration C_T can be determined using the mass balance. C_T and pK values, as well as their reproductibility error accuracy obtained for each sample are listed in table3. Then doing $\alpha_2 = 1$and $\alpha_0 = 0$, or *vice-versa*, in (11) the modulus of the saturation value of the surface charge density σ_0^{max} is calculated (see table 3).

Table 3. Triplicate values for sample A[3] and B. Total concentration of superficial sites C_T, pK's values of the weak acid superficial sites $pK_1(\equiv MOH_2^+)$ and pK_2 $(\equiv MOH)$, saturated surface charge density σ_0^{max}, pH value of isoelectric point and the respective reproducibility errors accuracy.

Sample	C_T(mol L^{-1})	pK_1	pK_2	$\lvert\sigma_{0\ \mathrm{max}}\rvert$(C m^{-2})	pH_{IEP}
	0.014	5.3	8.7	0.320	7.0
A	0.015	5.0	8.5	0.337	6.8
($CoFe_2O_4$)	0.014	5.2	8.6	0.320	6.9
	0.014 ± 0.001	5.2 ± 0.2	8.6 ± 0.1	0.326 ± 0.010	6.9 ± 0.1
	C_T(mol L^{-1})	pK_1	pK_2	$\lvert\sigma_{0\ \mathrm{max}}\rvert$(C m^{-2})	pH_{IEP}
	0.015	4.9	9.1	0.271	7.0
B	0.015	4.8	9.1	0.271	7.0
($MNFe_2O_4$)	0.014	4.9	9.2	0.270	7.1
	0.015 ± 0.001	4.9 ± 0.1	9.1 ± 0.1	0.271 ± 0.001	7.0 ± 0.1

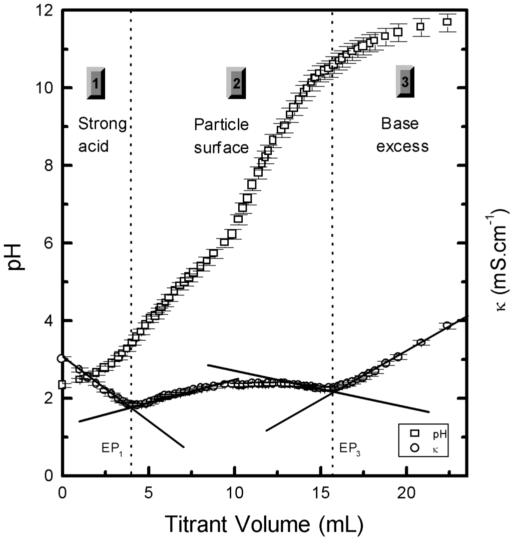

Figure 4. Simultaneous conductimetric-potentiometric titration curves of sample B. The regions indexed 1, 2 and 3 correspond to the strong acid titration (bulk solution), the weak acid $\equiv MOH_2^+$ and amphoteric $\equiv$ MOH superficial sites titrations and the base excess respectively. EP_1 and EP_3 are determined by the technique of graphical directions lines.

In Fig. 5, the molar ratio values of each particle surface site α_n calculated using (5) is plotted as a function of pH for sample B and represents a speciation diagram which illustrate the domains of protonation of surface sites. Sample B exhibits the same behavior that sample A [3]: at low (high) pH values or in acidic (basic) medium (typically pH $\leq$ 3.5 and pH $\geq$ 10.5, respectively), the particle surface is charge saturated. For small pH ranges around pK values, a domain of coexistence of charged and neutral sites is evidenced. Close to the neutral region, the molar ratio of charged sites strongly decreases and contrary to the expected result, the ferrofluid dispersion does not present any PZC since the molar ratio of the amphoteric sites does not reach the unity value. However, an isoelectric point (IEP) is found and is readily related to the equilibrium constants [3, 12] of the surface sites species. Once the pK values are known, the exact pH position of the IEP can be determined by mean of pK values, according to the Henderson-Hasselbach equation written in the case of equilibria (8) and (9). Table 3 lists the calculated pH_{IEP} for samples A [3] and B.

Finally, Figs. 6 show the pH dependence of σ_0 determined in the case of sample B. For extreme pH values (pH $\leq$ 3.5 and pH $\geq$ 10.5) σ_0 reaches the maximum and the particle surface becomes saturated. Then, for convenient ionic strength, stable magnetic sols are observed in acidic or basic mediums. Close to the IEP, the surface charge is very small to ensure a sufficient repulsion between particles and the ferrofluid dispersions are not longer stable.

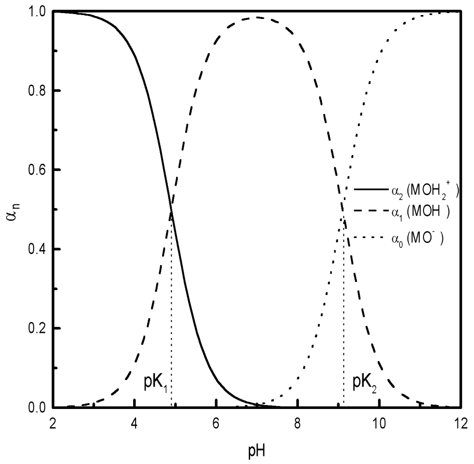

Figure 5. Speciation diagram of superficial sites for samples $B \cdot \alpha_n$ is the molar ratio of each superficial site, where n denotes the number of associated protons. For pH=7.0, there is an isolectric point.

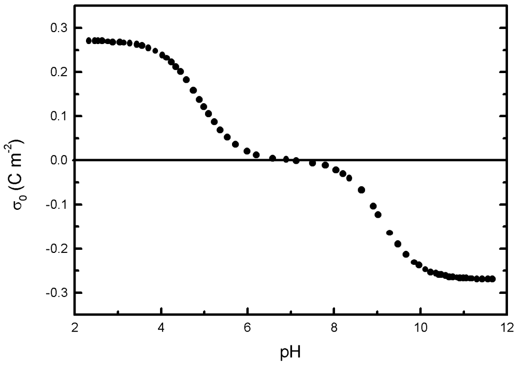

Figure 6. pH dependence of the superficial density of charge for sample B. For pH < 3.5 in acidic medium and pH > 10.5 in basic one, the nanoparticles are charge saturated and the ferroflui is thermodynamically stable (without considering ionic strength effects).

Figure 7 exhibits the three different states (sol, gel and floc) observed [7] for maghemite based EDL-MF diluted solution (ϕ = 1.45 %) and we add to this experimental phase diagram, the variation of the modulus of the surface charge density obtained in samples A [3] and B. Even if the magnetic fluids samples of our study are different (nanoparticle size and material) from those of reference 7, it can be observed that the pH dependent phase diagram is straightly related with the changes of the superficial density of charge. As expected, when the nanoparticle is charge saturated the observed phase is a stable sol and for low value of σ_0, in the region close to the IEP, the system flocculates. Moreover, the coincidence, in either acidic medium or basic one, of the gel phase with a regime of initial decreasing of the surface charge density has recently been explained by a charge sharing between particles [3]. It has been shown that a proton hopping (Grotthus Mechanism) along the hydrogen-bond network of liquid water adjacent to the particles can lead to a three dimensional strucuture. Indeed, this polimerization-like proccess results in relatively long-range interaction forces [16] and is already well known in many hydrophilic colloidal systems.

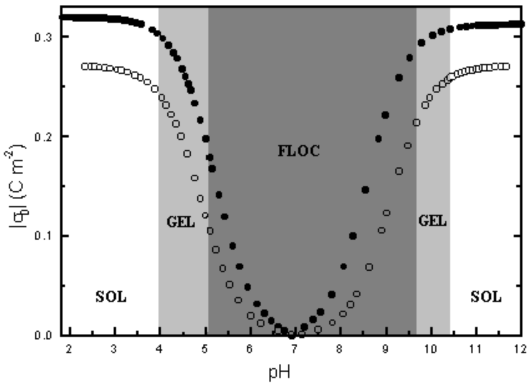

Figure 7. Modulus of the superficial density of charge in samples A [3] (•) and B (o). The dashed regions represent the different states observed for a maghemite based EDL-MF.

IV Conclusions

Simultaneous potentiometric and conductimetric titrations is proved to be a useful tool for the understanding of the behavior of mixtures of strong and weak acids when both the difference between the successive pK's is inferior to 4 and the second pK is superior to 8. Moreover, the colloidal stability of electrostatically stabilized ferrofluid dispersion can be quantitatively investigated by using these same measurements. For the first time, a model for the interface particle solution, where the particle surface behaves as a diprotic weak acid and the bulk solution as a strong one, is proposed and leads to saturation value of surface charge density in good agreement with the commonly reported one. The obtained results allows to relate the pH dependence of the phase diagram to the variations of the nanoparticle surface charge density and this method is therefore useful to monitor the colloidal stability of EDL-MF.

Acknowledgement

We acknowledge the Brazilian agencies FAP-DF, CAPES and CNPq.

References

[1] F.A. Tourinho, J. Depeyrot, G.J. da Silva, and M.C.L. Lara, Braz. J. of Phys. **28**, 413 (1998).

[2] J. N. Israelachvili, *Intermolecular and Surface Forces* (Academic Press, New York, 1985).

[3] A.F.C. Campos, F.A. Tourinho, G.J. da Silva, M.C.F.L. Lara, and J. Depeyrot, Eur. Phys. J. E. **6**, 29 (2001).

[4] J.-C. Bacri, R. Perzynski, D. Salin, V. Cabuil, and R. Massart, J. of Colloid Interf. Sci. **132**, 43 (1989).

[5] E. Dubois, V. Cabuil, F. Boué, J.-C. Bacri, and R. Perzynski, Progr. Colloid Polym. Sci. **104**, 173 (1997).

[6] J.-C. Bacri, R. Perzynski, D. Salin, V. Cabuil, and R. Massart, J. Magn. Magn. Mater. **85**, 27 (1990).

[7] E. Hasmonay, A. Bee, J.-C. Bacri, and R. Perzynski, J. Phys. Chem. B **103**, 6421 (1999).

[8] F.A. Tourinho, A.F.C. Campos, R. Aquino, M.C.F.L. Lara, and J. Depeyrot, J. Magn. Magn. Mater. in press.

[9] G.D. Christian, *Analytical Chenistry*, 4^{th} edn. (John Wiley & Sons, New York, 1986) p. 134.

[10] P.W. Atkins, *Physical Chemistry*, 5th edn. (Oxford University Press, Oxford, 1994) p. 301.

[11] E. Chromiak, Analyst **120**, 149 (1995).

[12] D.A. Skoog, D.M. West, and F. J. Holer, *Fundamentals of Analytical Chemistry*, (Saunders College Publishing, Orlando, 1996) p. 280.

[13] F. A. Tourinho, R. Franck, and R. Massart, J. Mater. Sci. **25**, 3249 (1990).

[14] W. Stumm and J. J. Morgan, *Aquatic Chemistry: An Introduction Emphasizing Chemical Equilibria In Natural Waters*, (J. Willey & Sons, New York, 1981).

[15] R. Itri, J. Depeyrot, F.A. Tourinho, and M.H. Sousa, Eur. Phys. J. E. **4,** 201 (2001).

[16] H.E. Stanley and J. Teixeira, J. Chem. Phys. **73**, 3404 (1980).